





Green Synthesis of Zinc Oxide Nanoparticles as a Promising Nanomedicine Approach for Anticancer, Antibacterial, and Anti-Inflammatory Therapies

Nahed Ahmed Hussien¹, Maha Abd El Fattah Khalil¹, Michael Schagerl², Sameh Samir Ali³

¹Department of Biology, College of Science, Taif University, Taif, 21944, Saudi Arabia; ²Department of Functional and Evolutionary Ecology, University of Vienna, Vienna, A-1030, Austria; ³Botany Department, Faculty of Science, Tanta University, Tanta, 31527, Egypt

Correspondence: Michael Schagerl; Sameh Samir Ali, Email michael.schagerl@univie.ac.at; samh_samir@science.tanta.edu.eg

Background and Aim: The rapid advancement of nanotechnology has opened new avenues for biomedical applications, particularly in antimicrobial, anti-inflammatory, and anticancer therapies. Green synthesis of zinc oxide nanoparticles (ZnO-NPs) using plant extracts offers an eco-friendly and biocompatible alternative to traditional chemical methods. This study explores the synthesis of ZnO-NPs using *Syzygium aromaticum* (clove) bud extract (CBE) and evaluates their multifaceted biomedical potential, including anticancer, antibacterial, and anti-inflammatory properties.

Methods: Clove bud extract-zinc oxide nanoparticles (CBE-ZnO-NPs) were synthesized and characterized using scanning electron microscopy (SEM), energy dispersive X-ray spectroscopy (EDX), Fourier-transform infrared spectroscopy (FTIR), dynamic light scattering (DLS), and Brunauer-Emmett-Teller (BET) analyses to confirm their size, morphology, elemental composition, and surface properties. The anticancer efficacy was tested against tongue carcinoma (HNO-97) cells using the sulforhodamine B (SRB) assay. Antibacterial activity was assessed against *Escherichia coli*, *Staphylococcus aureus*, *Pseudomonas aeruginosa*, and *Bacillus cereus*, while anti-inflammatory potential was evaluated using a mouse macrophage cell line (RAW 264.7).

Results: The SEM analysis confirmed a non-uniform shape of ZnO-NPs, while FTIR revealed functional groups responsible for stabilization and bioactivity. DLS measurements indicated an average particle size of 249.8 nm with a zeta potential of -3.38 mV, ensuring moderate colloidal stability. BET analysis demonstrated a high porosity (30.039 m²/g) and a mean particle size of 19.52 nm. CBE-ZnO-NPs exhibited moderate anticancer activity against tongue carcinoma cells ($IC_{50} > 100$ µg/mL), potent antibacterial activity ($MIC = 62.5$ – 125 µg/mL), and anti-inflammatory effects ($IC_{50} = 69.3$ µg/mL).

Conclusion: This study highlights the potential of CBE-ZnO-NPs as a promising multi-functional nanomaterial with potent antibacterial, anticancer, and anti-inflammatory properties. The findings pave the way for further exploration of ZnO-based nanotherapeutics in biomedical applications, particularly in cancer therapy, infection control, and inflammatory disorders.

Keywords: nanotechnology, green synthesis, zinc oxide nanoparticles, biomedical applications, *Syzygium aromaticum*

Introduction

The field of nanotechnology is rapidly advancing, particularly in the synthesis of nanoparticles derived from natural sources.^{1,2} This approach has the potential to revolutionize several industries, particularly in biomedicine and environmental applications.^{3,4} The shift toward utilizing sustainable, environmentally friendly, and cost-effective natural resources to produce nanoparticles offers numerous advantages, particularly in biological and medical applications where purity and safety are of utmost importance. Plant-derived nanoparticles, due to their non-toxic nature and ease of disposal, are becoming increasingly favored compared to those produced through traditional physicochemical methods.⁵ This green synthesis not only enhances the stability and efficacy of nanoparticles but also provides a sustainable alternative to conventional chemical manufacturing, which often requires harmful stabilizers and solvents.

Despite these benefits, the rate of synthesis of nanoparticles through biological means has not yet surpassed that of traditional methods,⁶ highlighting an area of continued research for optimizing production processes.

Among the various metallic nanoparticles, zinc oxide nanoparticles (ZnO-NPs) have garnered significant attention due to their versatility, stability, and broad-spectrum biomedical applications, including antimicrobial, anticancer, and anti-inflammatory activities.^{6–9} ZnO-NPs are widely utilized in drug delivery systems, diagnostics, biosensors, and therapeutic formulations owing to their low toxicity, high surface area, and ability to generate reactive oxygen species (ROS), which disrupt pathogenic microorganisms and cancerous cells.^{10,11} While traditional ZnO-NP synthesis relies on physical and chemical techniques, these methods often involve toxic stabilizers, harsh reaction conditions, and environmental concerns.¹² Consequently, the transition to “green synthesis” of ZnO-NPs using plant extracts has emerged as a promising alternative, offering enhanced biocompatibility and reducing toxic byproducts.^{13,14} Despite the well-documented biological activities of ZnO-NPs, there remains a pressing need for further investigation into their anti-inflammatory and anticancer mechanisms, particularly when synthesized using bioactive-rich plant extracts.^{15,16}

The increasing prevalence of antimicrobial resistance and the urgent need for novel therapeutic agents have accelerated research into medicinal plants as a source of bioactive compounds.¹⁷ Plants possess diverse phytochemicals with antimicrobial, anticancer, and anti-inflammatory properties, which, when integrated into nanoparticle synthesis, can significantly enhance the biological potential of the resulting nanomaterials.^{18,19} Among these medicinal plants, *Syzygium aromaticum* (clove) has demonstrated remarkable pharmacological properties due to its rich composition of bioactive compounds, including eugenol, flavonoids, tannins, and terpenoids.^{20,21} Clove extract has been widely recognized for its potent antimicrobial, antioxidant, and anti-inflammatory effects, making it an ideal candidate for the green synthesis of ZnO-NPs.^{22,23} The unique phytochemical profile of clove not only stabilizes the nanoparticles during synthesis but also functionalizes ZnO-NPs with additional therapeutic properties, thereby enhancing their biomedical efficacy.²⁴

The antibacterial activity of ZnO-NPs has been extensively documented, with studies demonstrating their ability to disrupt bacterial membranes, inhibit enzymatic pathways, and induce oxidative stress, leading to bacterial cell death.^{25,26} Prior research has indicated that reducing the size of ZnO-NPs enhances their antibacterial efficacy, as smaller nanoparticles exhibit increased surface reactivity and stronger interactions with microbial cells.²⁷ Reports have shown that ZnO-NPs effectively eliminate *Staphylococcus aureus*, *Escherichia coli*, *Pseudomonas aeruginosa*, and *Bacillus cereus*, underscoring their potential as alternative antimicrobial agents.^{7,9,10} While numerous studies have examined the antibacterial activity of ZnO-NPs, fewer investigations have explored the therapeutic implications of ZnO-NPs in cancer treatment and inflammation modulation, particularly when synthesized using biofunctionalized plant extracts.²⁸ The interaction between biosynthesized ZnO-NPs and cancerous cells remains an area of ongoing research, as ZnO-NPs can induce apoptosis, inhibit tumor growth, and modulate cellular oxidative stress, making them promising candidates for nanomedicine applications.^{29–31}

Despite recent investigations into the biosynthesis of ZnO-NPs using clove bud extract (CBE),²² their full therapeutic potential remains largely unexamined, particularly concerning their anti-cancer, antibacterial, and anti-inflammatory effects. Given the increasing global demand for biocompatible and multi-functional nanomaterials, the present study aims to biosynthesize and characterize ZnO-NPs using *Syzygium aromaticum* bud extract (CBE-ZnO-NPs) and systematically evaluate their antimicrobial, anticancer, and anti-inflammatory properties. Unlike previous studies that have primarily focused on antimicrobial applications, this research specifically examines the effects of CBE-ZnO-NPs on tongue carcinoma (HNO-97) cells, their potential role in inflammation suppression, and their bacterial inhibition mechanisms. The novelty of this study lies in its integrated exploration of multiple therapeutic applications of biosynthesized CBE-ZnO-NPs, paving the way for safer and more effective nano-based treatments in oncology, infection control, and inflammatory disorders. These findings will contribute to the advancement of plant-derived nanomaterials as potential next-generation biomedical agents, offering a sustainable and biocompatible alternative for clinical applications.

Materials and Methods

Bacterial and Cell Line Culture

The bacterial strains *Escherichia coli* ATCC 8739, *Staphylococcus aureus* ATCC 29213, *Pseudomonas aeruginosa* ATCC 9027, and *Bacillus cereus* ATCC 9634 were obtained from Nawah Scientific Inc. (Mokatam, Cairo, Egypt).

These strains were cultured in 100 mL of tryptic soy broth (TSB) composed of casein peptone (1.7 g), soy peptone (0.3 g), sodium chloride (0.5 g), dipotassium hydrogen phosphate (K_2HPO_4 , 0.25 g), and dextrose (0.25 g). The cultures were incubated at 37 °C for 24 hours to assess the antimicrobial activity of the biosynthesized CBE-ZnO-NPs. Ciprofloxacin and gentamicin (Oxoid, United Kingdom) were used as positive control antibiotics for comparison.

The HNO-97 and mouse macrophage (RAW 264.7) cell lines (Nawah Scientific Inc., Mokattam, Cairo, Egypt) were also used in this study. The HNO-97 cell line, derived from oral squamous cell carcinoma (OSCC),³² is widely used as an in vitro model to evaluate anticancer potential, particularly for assessing the cytotoxic effects of nanoparticles on OSCC. The HNO-97 cells were maintained in Dulbecco's Modified Eagle Medium (DMEM; Sigma-Aldrich, Merck Millipore)³³ supplemented with 100 units/mL penicillin, 100 µg/mL streptomycin (Oxoid, United Kingdom), and 10% heat-inactivated fetal bovine serum (FBS; Thermo Fisher Scientific, Gibco™ Brand). The cells were incubated in a humidified atmosphere containing 5% (v/v) CO_2 at 37 °C for 24 hours to ensure optimal growth conditions. Similarly, the RAW 264.7 cell line, derived from BALB/c mice, is a well-established in vitro model for macrophage research. The RAW 264.7 cells were cultured in DMEM supplemented with 10% FBS, 4 mm L-glutamine, 1 mm sodium pyruvate, and 4.5 g/L glucose.^{34,35} The cells were seeded in a 96-well microplate and incubated under the same conditions (37 °C, 5% CO_2) for 24 hours before further experimental procedures.

Preparation of Aqueous Extract from *Syzygium Aromaticum*

The collected clove (*Syzygium aromaticum*) buds were identified by Prof. Dr. Dalia A. Ahmed at Botany Department and the corresponding herbarium specimen was deposited in the Tanta University Herbarium (TANE) under the accession number TANE-14307. To prepare the CBE, dried clove blossoms were finely ground using an electric grinder. The grinding process was conducted in short pulses to prevent excessive heat generation, which could degrade the bioactive compounds.^{36–38} The powdered clove buds were then mixed with sterile distilled water at a 1:10 (w/v) ratio and gently simmered for 10 minutes to facilitate the extraction of bioactive components. The mixture was subsequently filtered to remove solid residues and allowed to cool at room temperature, yielding the CBE. The extract was stored under controlled conditions for further use.

Biosynthesis of CBE-ZnO-NPs

To synthesize CBE-ZnO-NPs (Supplementary Figure 1), 5 mL of clove bud extract (CBE) was mixed with 95 mL of 0.01 M zinc acetate dihydrate solution ($Zn(CH_3COO)_2 \cdot 2H_2O$) in sterile distilled water. The mixture was continuously stirred at 70°C for 1 hour, and the pH was adjusted to approximately 8 using 0.1 M NaOH to facilitate nanoparticle formation. The appearance of a granular brown precipitate during the reaction indicated the successful synthesis of ZnO-NPs.³⁹ The synthesized CBE-ZnO-NPs were then transferred to large glass Petri plates and allowed to dry overnight at 60°C to achieve complete desiccation, resulting in a dry powder for further evaluations.^{36,37}

Phytochemical Analysis

To analyze the phytochemical composition of the CBE, a methanolic extract was prepared. Dried clove buds were finely ground, and 200 mL of methanol was added for maceration, allowing the mixture to soak overnight to facilitate the extraction of bioactive compounds. The mixture was then filtered, and the residual solid material underwent a second round of maceration in methanol for one hour, followed by filtration. This extraction process was repeated twice to ensure the exhaustive extraction of phytoconstituents.⁴⁰ The final methanolic extract was concentrated and analyzed using gas chromatography-mass spectrometry (GC-MS) on a SHIMADZU QP2010 system (Japan), following the methodology previously described.⁴¹ GC-MS is widely recognized as one of the most efficient, precise, and rapid analytical techniques for identifying and quantifying bioactive compounds in plant extracts. The major phytochemicals identified in the CBE, such as phenolics, flavonoids, and terpenoids, play a critical role in the biosynthesis, capping, and stabilization of CBE-ZnO-NPs. These phytochemicals contain functional groups (eg, hydroxyl, carbonyl) that act as reducing and stabilizing agents during nanoparticle synthesis, thereby enhancing the biological properties of the resulting nanoparticles.

Characterization of Biosynthesized CBE-ZnO-NPs

The biosynthesized CBE-ZnO-NPs were characterized using multiple analytical techniques to evaluate their optical properties, structural composition, surface morphology, particle size, surface charge, and porosity. The surface morphology of the CBE-ZnO-NPs was analyzed using scanning electron microscopy (SEM; JEOL JSM-6390LA, Tokyo, Japan, EMU of Taif University) at an accelerating voltage of 20 kV. Prior to imaging, the nanoparticles were coated with a thin layer of gold using a Cressington Sputter Coater (108 Auto, thickness controller MTM-10, UK) for 10 minutes to enhance conductivity and prevent charging effects during SEM analysis.

The elemental composition of the synthesized CBE-ZnO-NPs was determined using EDX analysis (JEOL 6390LA). The EDX analysis was performed under the following acquisition conditions: accelerating voltage of 20.0 kV, process time and mode set to PHA Mode T3, live time of 25.81 seconds, real time of 28.88 seconds, dead time of 10%, counting rate of 2137 counts per second (cps), and an energy range of 0–20 keV.

Fourier-transform infrared spectroscopy (FTIR; PerkinElmer, USA) was employed to identify the functional groups present on the surface of the nanoparticles. These functional groups play a critical role in the stabilization and capping of the nanoparticles during biosynthesis.² The particle size distribution (PSD), polydispersity index (PDI), and Z-average diameter (nm) of the CBE-ZnO-NPs were determined using DLS measurements on a ZetaSizer Nano Series (HT), Nano ZS (Malvern Instruments, UK).^{42,43} The zeta potential of the nanoparticles was also measured using the same instrument, with water as the dispersing medium, to evaluate the colloidal stability of the nanoparticles.^{42,43}

The specific surface area, pore size, and porosity of the CBE-ZnO-NPs were evaluated using the Brunauer–Emmett–Teller (BET) method (Quantachrome, USA).⁴⁴ Approximately 0.3 g of the nanoparticles was placed in a BET analysis tube and degassed at 175 °C for 2 hours under nitrogen flow to remove adsorbed moisture and impurities. The mesoporous properties of the nanoparticles were further analyzed using the Barrett–Joyner–Halenda (BJH) method, which was applied to the N₂ adsorption-desorption isotherm data obtained using the Tristar 3000 system (Micromeritics Instrument Corp., Norcross, GA, USA).⁴⁵ Additionally, the micropore area was calculated using the t-plot method, providing detailed insights into the structural porosity of the CBE-ZnO-NPs.

Biological Applications of CBE-ZnO-NPs

Cytotoxicity and Anti-Cancer Analysis

The cytotoxic efficacy of CBE-ZnO-NPs and their half-maximal inhibitory concentration (IC₅₀) were evaluated in RAW 264.7 and HNO-97 cell lines using the SRB assay.⁴⁶ Briefly, cells were seeded at a density of 5×10^3 cells per well in 96-well plates containing Dulbecco's Modified Eagle Medium (DMEM) and incubated for 24 hours at 37°C in a humidified atmosphere with 5% CO₂. After incubation, the cells were treated with 100 µL of media containing varying concentrations of CBE-ZnO-NPs (0.05–500 µg/mL for RAW 264.7 and 0.01–100 µg/mL for HNO-97) and incubated for 72 hours. Following treatment, the cells were fixed by adding 150 µL of 10% trichloroacetic acid (TCA) to each well and incubating at 4°C for 1 hour. After fixation, the TCA solution was removed, and the cells were washed thoroughly with distilled water. Subsequently, 70 µL of a 0.4% (w/v) SRB solution was added to each well, and the plates were incubated at room temperature in the dark for 10 minutes. The plates were then washed three times with 1% acetic acid to remove unbound dye and allowed to dry overnight. To solubilize the protein-bound SRB dye, 150 µL of 10 mM TRIS buffer was added to each well. The absorbance of the solubilized dye was measured at 540 nm using a TECAN Infinite F50 microplate reader (Switzerland). The IC₅₀ values of CBE-ZnO-NPs for both cell lines were calculated to determine their cytotoxic potential.^{47,48}

Anti-Bacterial Activity

The bacterial strains *Escherichia coli* ATCC 8739, *Staphylococcus aureus* ATCC 29213, *Pseudomonas aeruginosa* ATCC 9027, and *Bacillus cereus* ATCC 9634 were cultured on tryptic soy agar.⁴⁹ The inoculum was prepared by incubating the plates at 37°C for 24 hours. The resulting bacterial cultures were suspended in sterile saline solution to achieve a final concentration of 1×10^6 CFU/mL.⁵⁰ For the broth microdilution assay, 100 µL of CBE-ZnO-NPs at a concentration of 1000 µg/mL was added to the first well of a 12-well plate. Each subsequent well was filled with 50 µL of Mueller-Hinton Broth (MHB; Sigma, St. Louis, MO, USA), followed by serial dilution to obtain nine different

concentrations ranging from 1000 to 1.953 µg/mL. To achieve a final bacterial concentration of 5.0×10^5 CFU/mL, 50 µL of the prepared inoculum was added to each well. Additionally, 50 µL of each bacterial strain suspension was diluted and cultured separately to confirm the inoculum density. Each plate included a growth control well (containing inoculated broth) and a negative control well (containing broth alone). The plates were incubated at 37°C for 24 hours. Ciprofloxacin and gentamicin were used as positive controls at concentrations ranging from 1000 to 1.953 µg/mL. The minimum inhibitory concentration (MIC) was determined as the lowest concentration of CBE-ZnO-NPs that inhibited visible bacterial growth. To complement the MIC results, the minimum bactericidal concentration (MBC) was also assessed. For MBC determination, 50 µL aliquots from wells showing no visible bacterial growth were plated onto agar plates and incubated at 37°C for 24 hours. The MBC endpoint was defined as the lowest concentration of CBE-ZnO-NPs that resulted in a 99.9% reduction in bacterial viability.⁵⁰

Anti-Inflammatory Assay

RAW 264.7 cells (1×10^5 cells/well) were cultured in DMEM, seeded into a 96-well microplate, and incubated for 24 hours at 37°C with 5% CO₂. The following day, inflammation was induced in the experimental group by treating the cells with 1 µg/mL of lipopolysaccharide (LPS), while the control group remained untreated and received only fresh media. Cells were then treated with varying concentrations of CBE-ZnO-NPs (0.05, 0.5, 5, 50, and 500 µg/mL). Quercetin (30 µM) was used as a positive anti-inflammatory control.^{46,51} Nitric oxide was quantified using ELISA plate reader and measuring absorbance at 540 nm.⁵²

Statistical Analysis

Data analysis was performed using GraphPad Prism 9.0. The bactericidal efficacy of antimicrobials was compared using one-way ANOVA. The mean and standard deviation (SD) of three independent replicates were calculated. Statistical significance was considered at a *P*-value of ≤ 0.05 .

Results and Discussion

Characterization of Biosynthesized Nanomaterials

Phytochemical screening of the clove bud extract (CBE) was performed using gas chromatography-mass spectrometry (GC-MS), as illustrated in Figure 1. Analysis of the CBE revealed six primary compounds, which were identified and organized based on their elution and retention times. The major component was eugenol (C₁₀H₁₂O₂), accounting for 45.46% of the composition, followed by eugenol acetate (42.73%), caryophyllene, palmitic acid methyl ester, oleic acid methyl ester, and arachidonic acid (Table 1). The chemical composition of the clove extract aligns with the eugenol-rich chemotype, as supported by numerous studies that have identified and quantified these components. For instance, *Syzygium aromaticum* extract from southern Brazil was reported to contain eugenol as the primary constituent (90.3%).⁵³ Similarly, Egyptian clove plants were found to contain eugenol (82.84%), acetyl eugenol (6.29%), and β-caryophyllene (8.13%).⁵⁴ In cloves collected from India, eugenol was documented as the major component, constituting 50% of the extract.⁵⁵ The variations in eugenol content and overall composition of clove extracts can be attributed to the geographical origin of the plant. These differences are likely influenced by biotic and abiotic factors, such as seasonal variations, developmental stages, plant age, and climatic conditions.⁵⁵

In this study, green synthesis of ZnO-NPs was achieved using *Syzygium aromaticum* bud extract. Visual inspection of the reaction mixture confirmed the formation of ZnO-NPs. Prior to incubation, the extract appeared as a clear brown solution; however, upon the addition of zinc acetate (precursor), the color changed to dark brown, indicating the reduction of Zn²⁺ ions to ZnO-NPs³⁷ (Figure S1). The synthesis process yielded 3.25 g of ZnO-NPs, which were subsequently used for further characterization and analysis. In the CBE, eugenol (45.46%) serves as a crucial stabilizing agent, preventing nanoparticle agglomeration and ensuring the formation of well-defined ZnO-NPs. Caryophyllene (8.14%) may act as a capping agent, directing the growth and morphology of the nanoparticles. Additionally, other components, such as eugenol acetate (42.73%), contribute to enhancing the biological activities of the synthesized nanoparticles. This diverse phytochemical composition enables the efficient and controlled synthesis of ZnO-NPs with tailored properties.²² SEM images of the biosynthesized CBE-ZnO-NPs revealed the formation of irregularly shaped

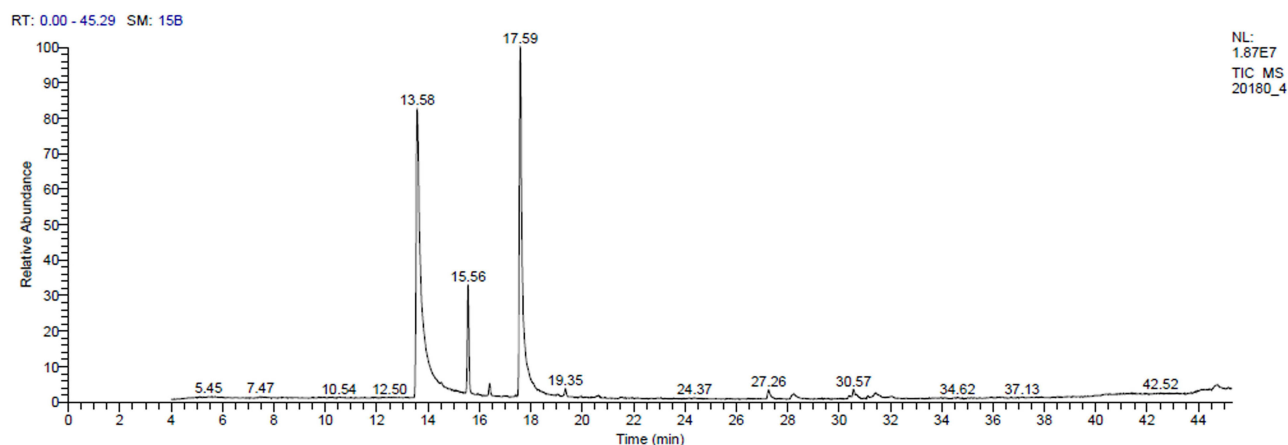


Figure 1 Chromatogram of *Syzygium aromaticum* bud extract obtained through GC-MS, illustrating the major phytochemical components.

nanoparticles with non-uniform size distribution, as shown in [Figure 2A](#). EDX analysis further confirmed the presence of zinc as the primary elemental component, along with significant amounts of carbon and oxygen on the nanoparticle surface ([Figure 2B](#)). The presence of carbon and oxygen is attributed to the organic compounds derived from the CBE, which was used as a reducing and stabilizing agent during the synthesis process.³⁷

Table 1 Phytochemical Composition of *Syzygium Aromaticum* Buds Extract

| Peak | RT | Area % | MW | Compound Name | Molecular Formula | Structure |
|------|-------|--------|-----|---|--|-----------|
| 1 | 13.58 | 45.46 | 164 | Eugenol | C ₁₀ H ₁₂ O ₂ | |
| 2 | 15.56 | 8.14 | 204 | Caryophyllene | C ₁₅ H ₂₄ | |
| 3 | 17.59 | 42.73 | 206 | Phenol, 2-methoxy-4-(2-propenyl)-, acetate (Eugenol acetate) | C ₁₂ H ₁₄ O ₃ | |
| 4 | 19.35 | 0.68 | 304 | Arachidonic acid | C ₂₀ H ₃₂ O ₂ | |
| 5 | 27.26 | 1.18 | 270 | Hexadecanoic acid, methyl ester (Palmitic acid, methyl ester) | C ₁₇ H ₃₄ O ₂ | |
| 6 | 30.56 | 0.86 | 296 | 11-Octadecenoic acid, methyl ester (Oleic acid, methyl ester) | C ₁₉ H ₃₆ O ₂ | |

Abbreviations: RT, retention time; MW, molecular weight.

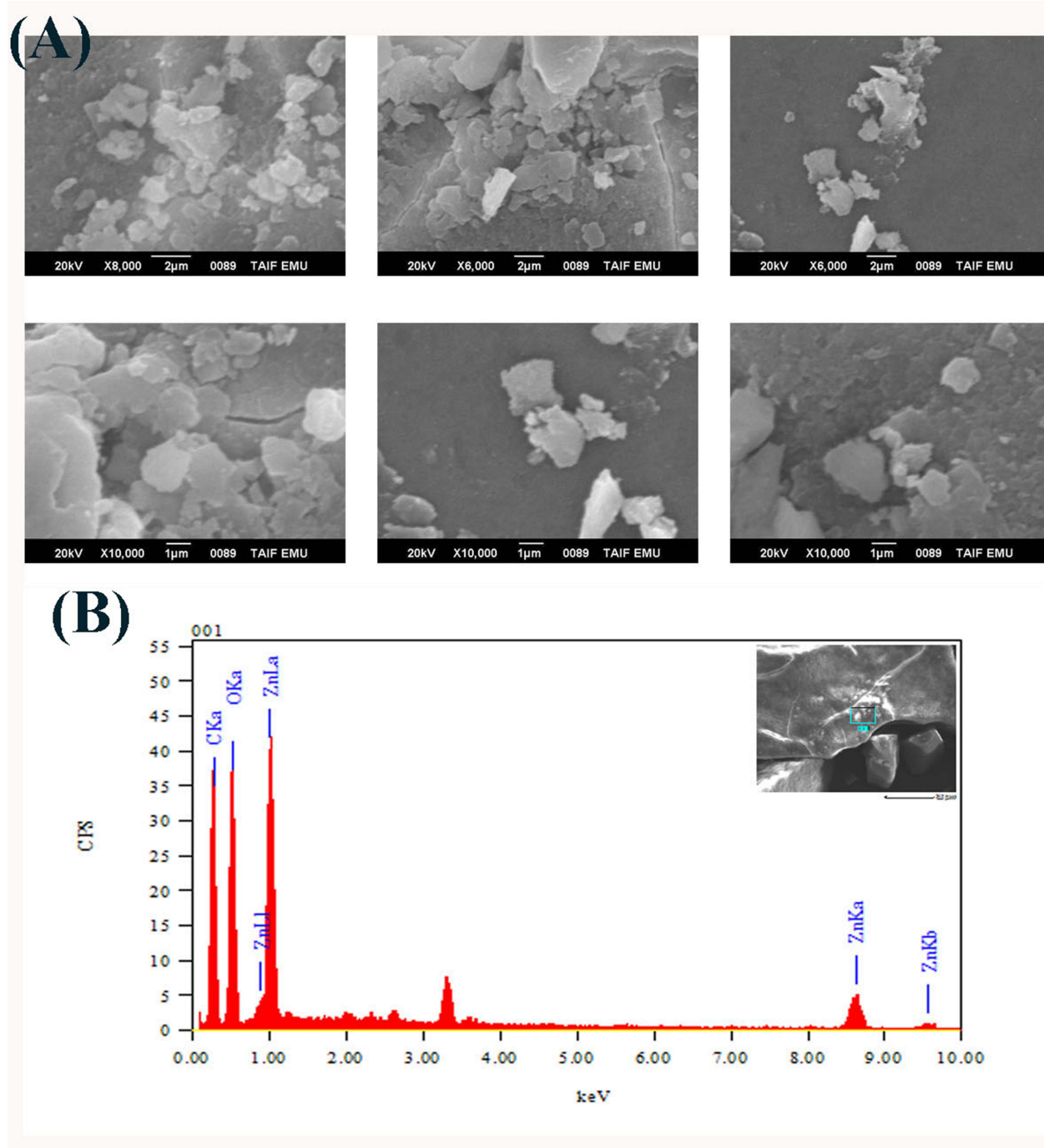


Figure 2 Photomicrograph showing the surface morphology of the biosynthesized CBE-ZnONPs by SEM (A) and the main composition on their surfaces using EDX (B).

The distinct signals observed in FTIR arise from substance-specific molecular vibrations. FTIR spectra of the CBE and CBE-ZnO-NPs were recorded in the range of 400–4000 cm^{-1} (Figure 3A and B). The FTIR spectra of CBE-ZnO-NPs exhibited several distinct peaks compared to the CBE extract alone (Table 2). In this regard, a broad peak at 3242 cm^{-1} was attributed to the N–H stretching vibration and overlapped with the O–H stretching vibration of hydroxyl groups.^{56,57} Absorbance peaks at 2922 cm^{-1} were consistent with C–H stretching vibrations.⁵⁸ The bands observed at 1558 cm^{-1} were assigned to C=O functional groups present in the samples. The peak around 1401 cm^{-1} corresponded to C=C stretching in aromatic rings, C=O stretching in polyphenols, and C–N stretching of amide-I in proteins. Bands at 1341 cm^{-1} were associated with C–H asymmetric vibrations. Peaks at 1192 and 1021 cm^{-1} were identified as C–O stretching vibrations, while a peak at 752 cm^{-1} was linked to C–H bending

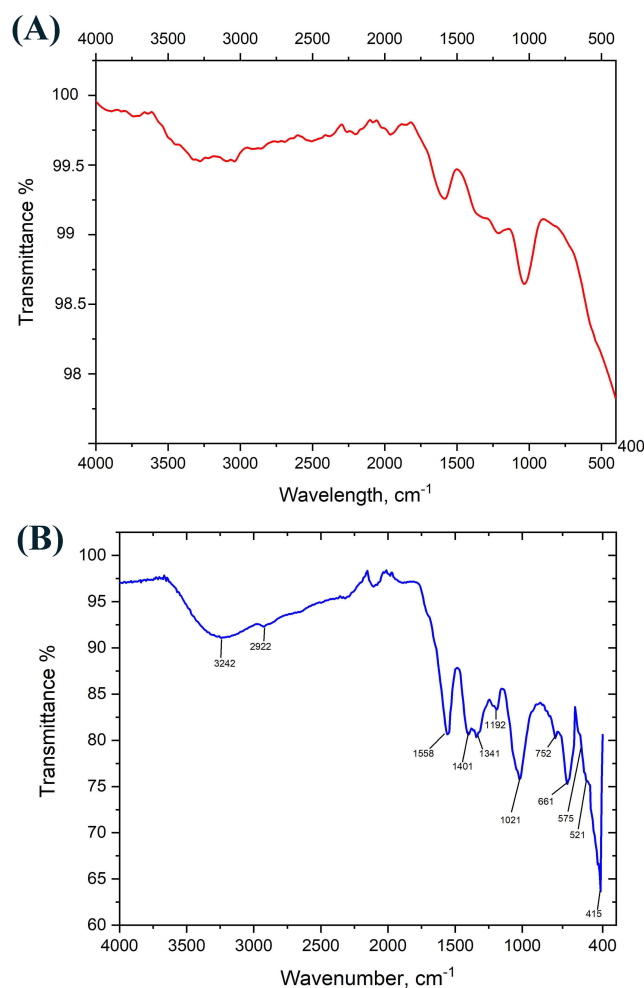


Figure 3 FTIR spectra of CBE (A) and biosynthesized CBE-ZnO-NPs (B), highlighting the functional groups responsible for nanoparticle stabilization and bioactivity.

vibrations. A distinct absorption band at 415 cm^{-1} confirmed the successful formation of ZnO, with the $400\text{--}600\text{ cm}^{-1}$ region representing ZnO stretching vibrations.⁵⁹ The appearance of additional absorption bands in the FTIR spectra, beyond the characteristic Zn-O stretching, can be attributed to several factors. One key factor is surface functionalization or adsorption. When nanoparticles are synthesized using plant extracts, biomolecules such as proteins, polyphenols, and flavonoids from the extract may cap the nanoparticle surface. These organic compounds introduce additional absorption bands corresponding to

Table 2 FTIR Analysis of CBE-ZnO-NPs

| No | Absorption Peak (cm^{-1}) in ZnO-NPs | Bond/Functional Groups |
|-----|---|---|
| 1. | 3242.78 | OH stretching vibrations |
| 2 | 2922.23 | C-H stretching |
| 3. | 1558.02 | C=C stretch in aromatic ring and C=O stretch in polyphenols |
| 4. | 1401.47 | C – N stretch of amide-I in protein |
| 5. | 1341.84 | C-H asymmetric vibration |
| 6. | 1192.74 | C–O stretching vibration |
| 7. | 1021.29 | C–O stretching vibration |
| 8. | 752.92 | C–H bending vibration |
| 9. | 661.90 | C- alkyl chloride |
| 10. | 575.01 | Hexagonal phase ZnO |
| 11. | 415.572 | ZnO |

functional groups like C=O (carbonyl), O-H (hydroxyl), C-N (amine), and C=C (aromatic rings). Additionally, ZnO nanoparticles often exhibit structural defects, such as oxygen vacancies or zinc interstitials, which can introduce new vibrational modes not present in bulk ZnO. The presence of residual water or hydroxyl groups adsorbed on the nanoparticle surface can also result in absorption bands, particularly in the 3300–3500 cm^{-1} region (O-H stretching) and around 1600 cm^{-1} (H-O-H bending). Furthermore, a metallic group signal at 575 cm^{-1} in the FTIR spectrum of the synthesized adsorbent confirms the presence of ZnO.⁶⁰ The adsorption process was facilitated by functional groups such as N-H, O-H, C=C, and C-O present in the sample.⁶¹ Sharp peaks at 661.90 and 575.01 cm^{-1} were attributed to C-alkyl chloride and the hexagonal phase of CBE-ZnO-NPs, respectively.⁶² The presence of various functional groups in the CBE, particularly phenolic compounds, likely facilitated the biological reduction of Zn^{2+} ions to CBE-ZnO-NPs. Additionally, carboxylic and phenolic acid groups played a crucial role in the bio-capping and stabilization of the synthesized ZnO-NPs.³⁷

The DLS technique was used to analyze the size distribution by number and zeta potential of the biosynthesized CBE-ZnO-NPs. The zeta potential, which measures the surface charge of colloidal particles, is a key indicator of their stability. Colloidal suspensions are generally considered stable if the zeta potential exceeds 15 mV.⁶³ As shown in the size distribution by number graph (Figure 4A), the average size of CBE-ZnO-NPs was 249.8 nm, indicating the presence of polydisperse, larger particles. The

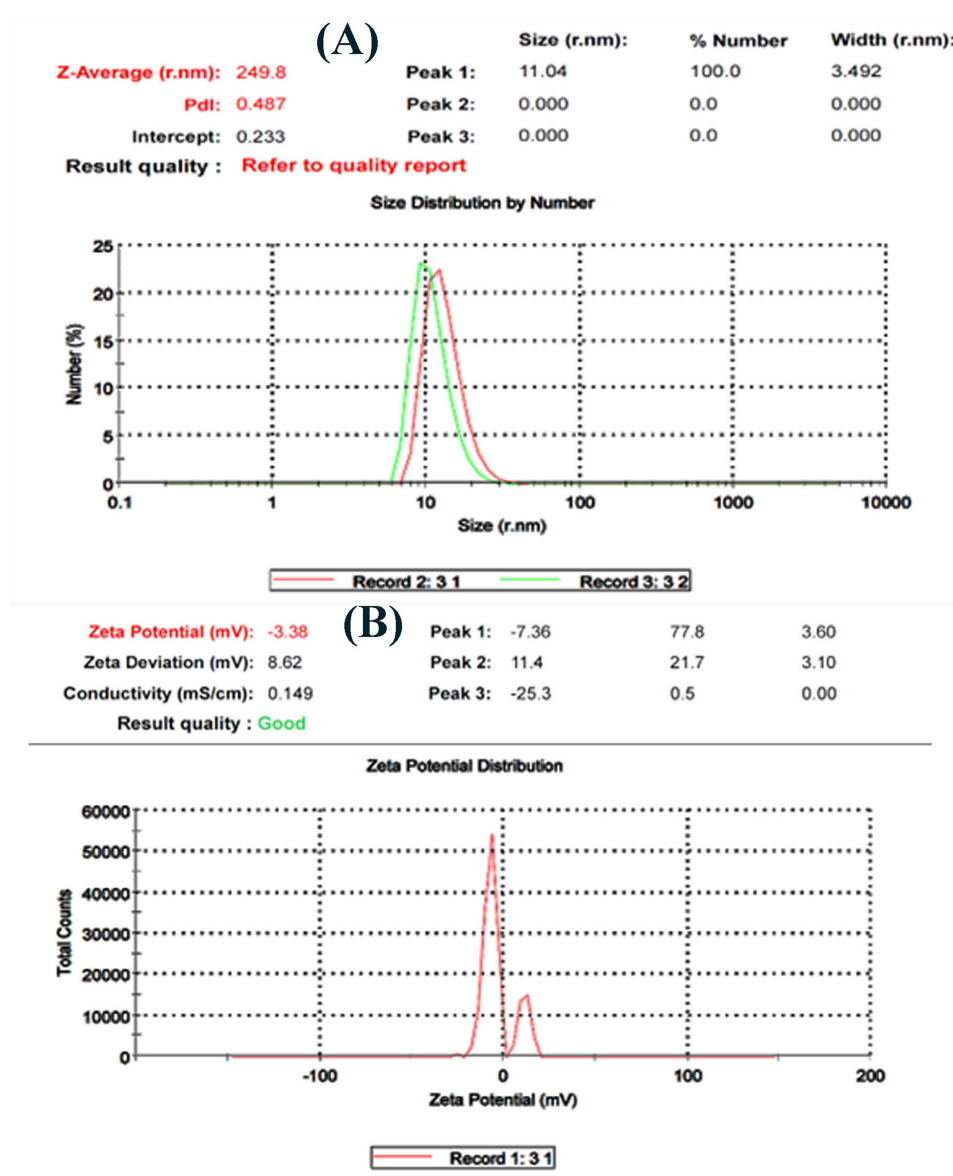


Figure 4 Particle size distribution by number (A) and zeta potential distribution (B) of CBE-ZnO-NPs, as determined by DLS.

PSD profile of the ZnO-NPs displayed a single prominent peak with 100% intensity. The PDI of the ZnO-NPs was 0.487,⁶⁴ which is consistent with values reported in several studies that consider PDI values below 0.5 to indicate a monodisperse system.^{65,66} The larger size of ZnO-NPs detected by DLS can be attributed to the technique's bias toward identifying larger particles or aggregates.⁶⁷ This bias may arise from the influence of functional groups such as carbohydrates, polysaccharides, and pectin adsorbed on the nanoparticles from the plant extract, which can affect the zeta potential and hydrodynamic size. The slightly larger hydrodynamic size observed in DLS measurements is likely due to the formation of a hydrodynamic shell around the nanoparticles, influenced by factors such as particle shape, surface texture, and composition.⁶⁸ These results remain within acceptable error limits. The zeta potential of the ZnO-NPs in distilled water was measured at -3.38 mV (Figure 4B), suggesting that the colloidal suspension is relatively stable. The negative surface charge is attributed to the binding of metabolites from the clove bud extract to the nanoparticles, which helps stabilize the ZnO-NPs and reduce their tendency to aggregate. This finding confirms the dispersive capacity of the environmentally synthesized ZnO-NPs.⁶⁹

The specific surface area of the ZnO-NPs synthesized from CBE was determined using the BET method, with nitrogen adsorption conducted at 170°C . Figure 5 illustrates the nitrogen adsorption-desorption isotherms for the CBE-ZnO-NPs. According to the IUPAC classification, the isotherm can be categorized as Type IV, and the hysteresis loops are classified as Type H3, which is characteristic of mesoporous materials.⁴⁴ The adsorption isotherm of the synthesized ZnO-NPs showed a gradual increase in adsorbed volume at low relative pressures (approximately 0.06 to 0.6), followed by a sharp rise at relative pressures above 0.6, as depicted in Figure 5. This behavior is consistent with findings reported previously.^{44,70} The BET analysis revealed a specific surface area of $30.039\text{ m}^2/\text{g}$, a pore volume of $0.1446\text{ cm}^3/\text{g}$, and an average particle size of 19.52 nm for the ZnO-NPs. The discrepancy between the BET results and the DLS measurements can be attributed to the rough and porous surface of the nanoparticles, which affects the BET analysis. Unlike DLS, which measures hydrodynamic size and is influenced by agglomeration, the BET method provides information on the size of non-agglomerated particles. Figure 6 shows the BJH pore size distribution for the synthesized CBE-ZnO-NPs. The distribution clearly indicates that the majority of pores

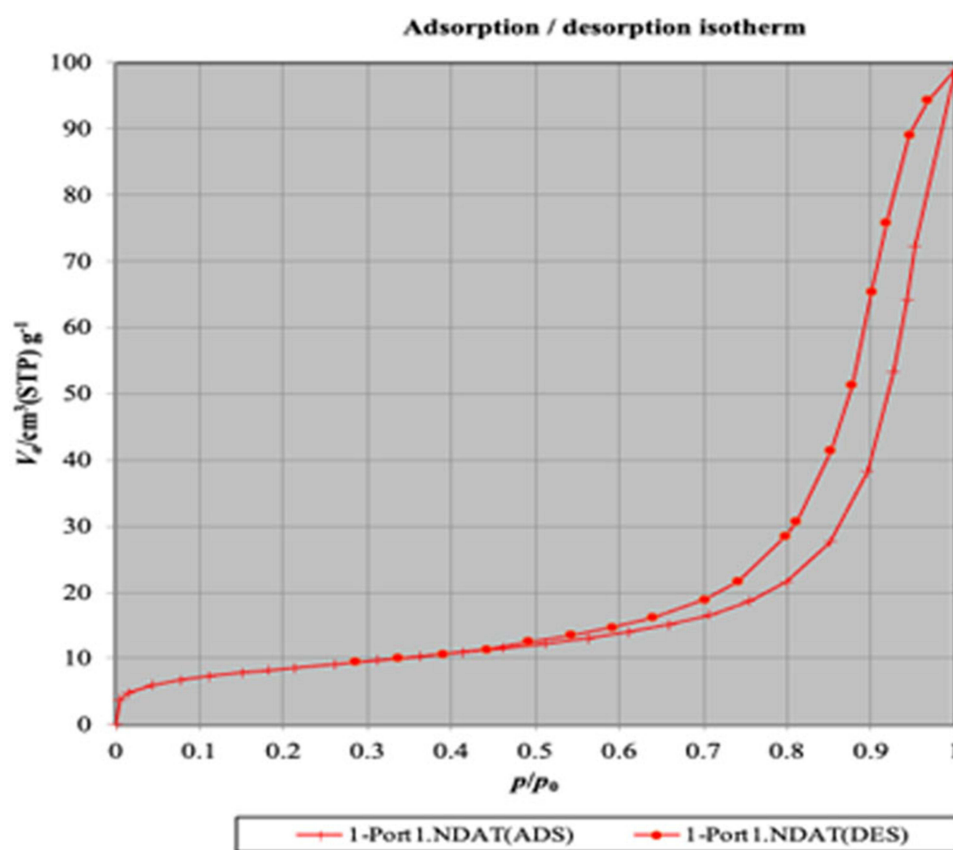


Figure 5 Nitrogen adsorption-desorption isotherms of CBE-ZnO-NPs, demonstrating the mesoporous nature of the nanoparticles.

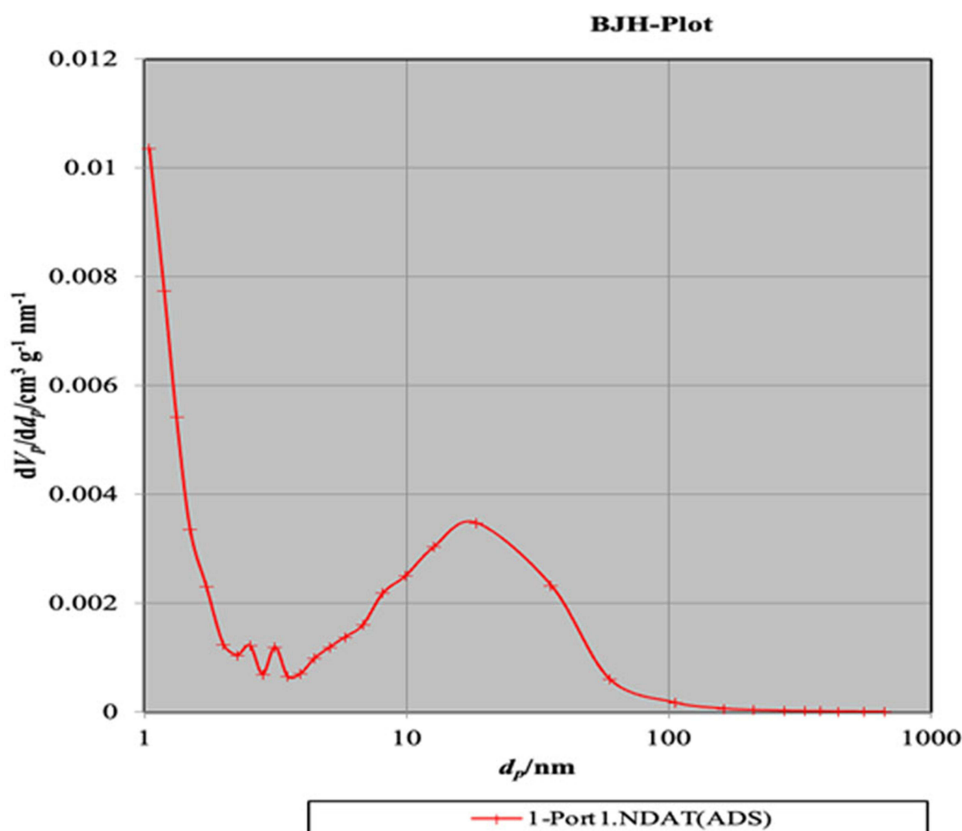


Figure 6 Barrett-Joyner-Halenda (BJH) pore size distribution of CBE-ZnO-NPs, showing the majority of pores within the 2–50 nm range.

fall within the 2–50 nm range, confirming the mesoporous nature of the material. This finding aligns with the Type IV adsorption isotherm and is consistent with previous studies.^{70,71}

Biological Activities

Cytotoxicity and Anti-Cancer Activities

Green synthesis is an eco-friendly and cost-effective approach that enhances production efficiency and improves biocompatibility for human applications. Utilizing natural compounds for biofabrication not only stabilizes nanoparticles but also reduces toxicity and enhances their reduction potential. The cytotoxicity of CBE-ZnO-NPs at concentrations ranging from 0.05 to 500 µg/mL was evaluated on RAW 264.7 cells using the SRB assay. The results demonstrated a concentration-dependent reduction in RAW 264.7 cell viability, with an IC₅₀ value of 382.85 µg/mL (Figure 7). These findings align with the study reported that *Syzygium aromaticum* bud extracts significantly inhibited RAW 264.7 cell activation at concentrations between 50 and 200 µg/mL.⁷²

The anticancer potential of CBE-ZnO-NPs was also assessed on HNO-97 cells using the SRB assay. The nanoparticles were tested at concentrations ranging from 0.01 to 100 µg/mL, and the response of the cancer cell line was found to be concentration-dependent. CBE-ZnO-NPs exhibited a marginal reduction in the metabolic activity of tumor cells at lower concentrations, with a more pronounced decline at higher concentrations. The IC₅₀ value for CBE-ZnO-NPs on HNO-97 cells was determined to be 73.35 µg/mL (Figure 8). This result is comparable to the IC₅₀ value reported for pomegranate peel-treated cell lines but significantly lower than that of blueberry dry powder (525.38 µg/mL).⁷³ The anticancer activity of CBE-ZnO-NPs is likely due to the presence of bioactive molecules from the clove extract adsorbed onto the nanoparticle surface, which enhance their therapeutic potential.

The dose-dependent anticancer effects of CBE-ZnO-NPs, as illustrated in Figure 8, highlight their potential as a promising therapeutic agent. Nanoparticles enhance bioavailability, enable targeted delivery, improve stability, and increase tissue-specific effects, thereby enhancing therapeutic efficacy and safety.⁷⁴ ZnO is widely used in modern drug

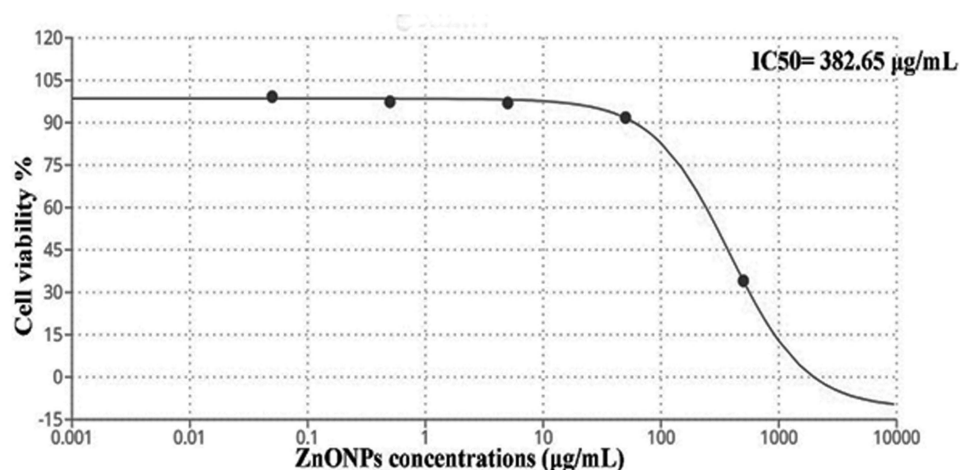


Figure 7 Effect of CBE-ZnO-NPs on the viability of RAW 264.7 cells, with the half-maximal inhibitory concentration (IC_{50}) determined using the SRB assay.

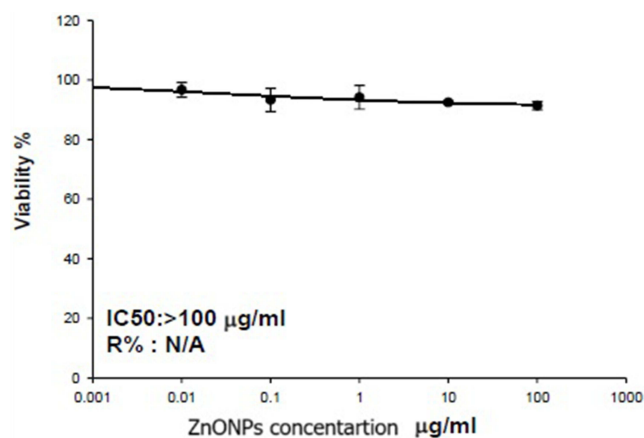


Figure 8 Anticancer activity of CBE-ZnO-NPs on the HNO-97 cell line, illustrating the concentration-dependent reduction in cell viability.

delivery systems due to its ease of synthesis, low cost, tunable structures, low toxicity, high drug-carrying capacity, and ability to facilitate controlled and targeted drug release.⁷⁵ Porous ZnO nanostructures, such as nanotubes, nanobelts, nanorods, and nanocages, are particularly effective in selective drug delivery systems.⁷⁶ The anticancer effect of ZnO-NPs is largely dependent on their ability to generate a sufficient amount of ROS, leading to DNA damage, lipid peroxidation, and protein dysfunction, ultimately causing cell death.⁷⁷ This mechanism is facilitated by the broad semiconductor properties of ZnO. As a wide bandgap semiconductor, ZnO, when exposed to ultraviolet or visible light, undergoes electron excitation from the valence band to the conduction band, leaving behind positively charged holes (h^+). These electrons and holes participate in redox reactions with oxygen and water molecules on the ZnO surface, resulting in the production of highly reactive ROS.⁷⁷ The pro-inflammatory response and redox reactions triggered by ZnO-NPs contribute to apoptotic cell death.⁷⁸ However, distinguishing between cancerous and normal cells remains a significant challenge in classifying a substance as anticancer.⁷⁹ A lack of selectivity can lead to systemic toxicity. Notably, several studies have demonstrated that ZnO-NPs exhibit selective cytotoxicity toward cancer cells. For instance, ZnO-NPs have been shown to preferentially kill Jurkat cancer cells while causing minimal damage to normal $CD4^+$ T cells.⁸⁰ ZnO-NPs exhibit 28–35 times greater cytotoxicity against malignant cells compared to normal cells.⁸¹ This selectivity is attributed to the enhanced permeability and retention effect, which allows nanoparticles to accumulate preferentially in tumor tissues due to their leaky vasculature and poor lymphatic drainage. Additionally, the electrostatic properties of ZnO-NPs enhance their targeting efficiency toward tumor cells.⁷⁵ A growing body of evidence supports the

potential of ZnO-NPs as a promising anticancer agent for various types of tumor cells. Their ability to selectively target cancer cells while minimizing damage to normal cells makes them a valuable candidate for cancer therapy.

Antibacterial Activity and Mechanisms of Action

The antibacterial activity of CBE-ZnO-NPs was evaluated against several reference strains: *Escherichia coli* ATCC 8739, *Staphylococcus aureus* ATCC 29213, *Pseudomonas aeruginosa* ATCC 9027, and *Bacillus cereus* ATCC 9634, at concentrations ranging from 1000 to 1.953 µg/mL (Figure S2). As shown in Table 3, the MIC values of CBE-ZnO-NPs ranged from 62.5 to 125 µg/mL, while the MBC values ranged from 125 to 1000 µg/mL. Notably, CBE-ZnO-NPs exhibited significant antibacterial activity against *Bacillus cereus* ATCC 9634 (MIC = 6.25 µg/mL, MBC = 125 µg/mL) and *Pseudomonas aeruginosa* ATCC 9027 (MIC = 125 µg/mL, MBC = 1000 µg/mL). In comparison, the positive controls, ciprofloxacin and gentamicin, demonstrated MIC values of less than 1.93 µg/mL and MBC values of less than 1.95 µg/mL for all tested strains, except for *Staphylococcus aureus* ATCC 29213, which had a MIC of 31.25 µg/mL. None of the CBE-ZnO-NP concentrations exhibited greater antibacterial potential than the positive controls, which served as effective benchmarks (Table 3). The antibacterial activity of CBE-ZnO-NPs was dose-dependent, and these findings align with previous studies on biosynthesized ZnO-NPs.⁸²

The strong bactericidal properties of CBE-ZnO-NPs are likely attributed to the bioactive compounds adsorbed onto their surface. These nanoparticles represent a promising alternative to conventional antibacterial agents due to their broad-spectrum physicochemical properties, which enable them to act through multiple mechanisms.⁸ As illustrated in Figure 9, the antibacterial activity and mechanism of action of CBE-ZnO-NPs are strongly influenced by oxidative stress. These include the disruption of bacterial cell membranes, interference with enzyme pathways, DNA and RNA polymerase inhibition, folic acid disruption, and impairment of protein synthesis.^{36,83} Zn²⁺ ions have been shown to reduce the activity of respiratory enzymes.⁸⁴ ZnO-NPs can degrade bacterial cell membranes and generate ROS, such as O₂^{•-}, H₂O₂, and OH[•]. These ROS can impair enzyme function, induce oxidative stress, and promote cell death by facilitating the uptake of Zn²⁺ ions, which further generate ROS free radicals capable of damaging DNA and cell membranes.⁸⁵ Additionally, the internalization of ZnO-NPs disrupts the energy metabolism of bacterial cells.⁸⁶ The ROS generated by ZnO-NPs can break the chemical bonds of bacterial organic matter, contributing to their bactericidal effect. While negatively charged peroxides cannot penetrate the cell membrane, OH⁻ ions accumulate on the membrane surface, leading to its destruction. In contrast, H₂O₂ can penetrate the cell membrane, causing damage to both the membrane and intracellular components. The physicochemical properties of ZnO-NPs may also hinder bacterial growth by interfering with DNA and plasmid replication, membrane depolarization, protein leakage, structural changes, and increased membrane fluidity.⁸⁷ These mechanisms collectively enhance the bactericidal potential of CBE-ZnO-NPs.

Anti-Inflammatory Activity

Inflammation is a complex physiological response to environmental toxins and plays a significant role in the development of chronic diseases.⁸⁸ In this study, RAW 264.7 cells were used to evaluate the anti-inflammatory potential of CBE-ZnO-NPs as a therapeutic agent. As shown in Figure 10, cell viability ranged from 99.18% at 0.05 mg/mL CBE-ZnO-NPs to 34.07% at 500 mg/mL. The anti-inflammatory activity was assessed by measuring the suppression of nitric oxide

Table 3 Antibacterial Activity of CEB- ZnO-NPs

| Bacterial Strains | Tested Antimicrobials (µg/mL) | | | | | |
|---|-------------------------------|------|------------|-------|---------------|-------|
| | CBE-ZnO-NPs | | Gentamycin | | Ciprofloxacin | |
| | MIC | MBC | MIC | MBC | MIC | MBC |
| <i>Escherichia coli</i> ATCC 8739 | 250 | 1000 | <1.95 | <1.95 | <1.95 | <1.95 |
| <i>Staphylococcus aureus</i> ATCC 29213 | 250 | 1000 | <1.95 | <1.95 | <1.95 | 31.25 |
| <i>Pseudomonas aeruginosa</i> ATCC 9027 | 125 | 1000 | <1.95 | <1.95 | <1.95 | <1.95 |
| <i>Bacillus cereus</i> ATCC 9634 | 62.5 | 125 | <1.95 | <1.95 | <1.95 | <1.95 |

Abbreviations: MIC, minimum inhibitory concentration; MBC, minimum bactericidal concentration.

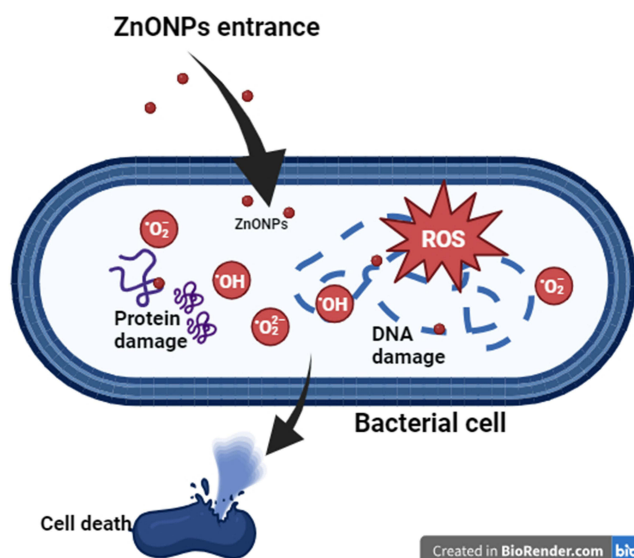


Figure 9 Proposed antibacterial action mechanism of CBE-ZnO-NPs, including ROS generation, membrane disruption, and inhibition of bacterial enzymatic pathways (Agreement number: ZX283CM23B).

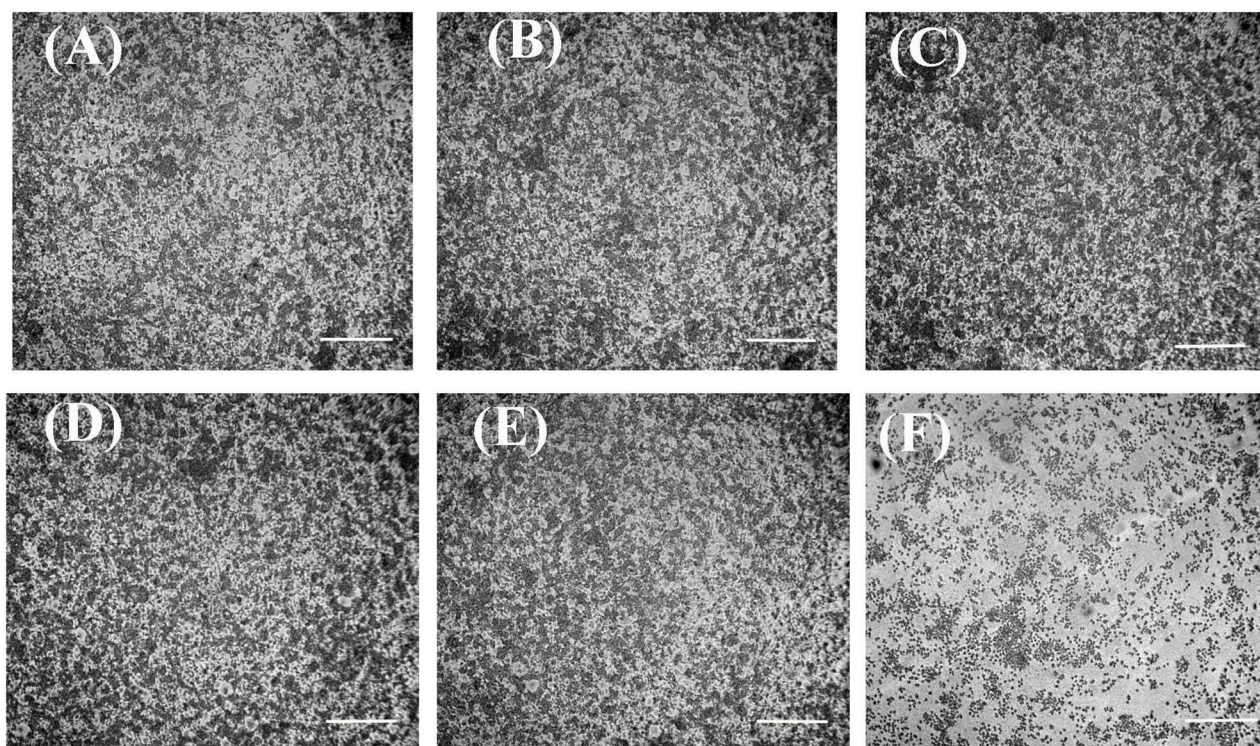


Figure 10 Anti-inflammatory efficacy of CBE-ZnO-NPs on LPS-induced RAW 264.7 cells. (A) Control; (B–F) RAW 264.7 cells treated with varying concentrations of CBE-ZnO-NPs: (B) 0.05 $\mu\text{g/mL}$, (C) 0.5 $\mu\text{g/mL}$, (D) 5 $\mu\text{g/mL}$, (E) 50 $\mu\text{g/mL}$, (F) 500 $\mu\text{g/mL}$. Scale bar = 200 μm .

production in LPS-induced RAW 264.7 cells, with an IC_{50} value of 69.3 $\mu\text{g/mL}$ (Figure 11). These findings indicate that CBE-ZnO-NPs enhance cytotoxicity in RAW 264.7 cells, thereby improving anti-proliferative capabilities. It has been reported that eugenol, an active compound in clover buds, exhibits significant anti-inflammatory properties.⁸⁹ The activation of macrophages is intricately linked to various illnesses due to their central role in immune responses.⁹⁰ As innate immune cells, macrophages primarily defend the host by performing phagocytic actions against foreign invaders.⁹¹ When activated, macrophages amplify both acute and chronic inflammatory responses by producing excessive oxidative

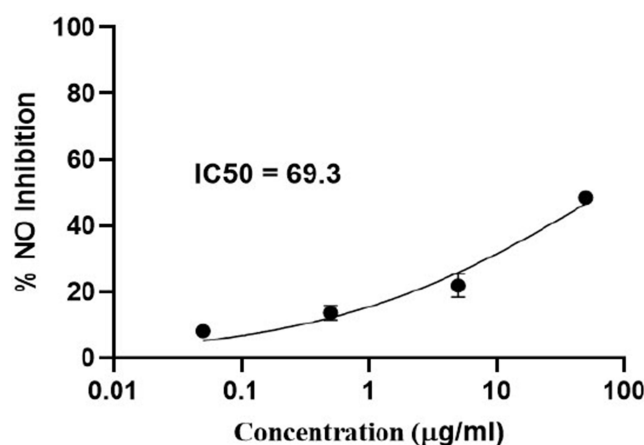


Figure 11 Effect of CBE-ZnO-NPs on the inhibition of nitric oxide (NO) production in LPS-induced RAW 264.7 cells, demonstrating their anti-inflammatory potential.

stress mediators, such as ROS, nitric oxide, and inflammatory cytokines.⁹² Over the past few decades, nanoparticles have emerged as promising anti-inflammatory agents. Their unique properties, including a high surface area-to-volume ratio, enable them to interact effectively with biological membranes and traverse them. The nanoscale size of ZnO-NPs facilitates their absorption across biological membranes. Research has demonstrated that ZnO-NPs can significantly reduce inflammation.⁹³ These nanoparticles exert their anti-inflammatory effects through multiple mechanisms, including the inhibition of myeloperoxidase, suppression of mast cell degranulation, downregulation of the NF- κ B pathway,⁹⁴ reduction of pro-inflammatory cytokine production, and decreased expression of inducible nitric oxide synthase.⁹⁵

Conclusions

This study successfully demonstrates the green synthesis of ZnO-NPs using *Syzygium aromaticum*, showcasing their potential as a versatile nanomaterial with significant biomedical applications. The biosynthesized CBE-ZnO-NPs exhibited promising antibacterial activity against both Gram-positive and Gram-negative bacteria, with MIC values ranging from 62.5 to 125 µg/mL, highlighting their potential as an alternative to conventional antibiotics in combating microbial resistance. Furthermore, the nanoparticles demonstrated moderate anticancer activity against HNO-97 cells, with an IC₅₀ value exceeding 100 µg/mL, suggesting their potential role in cancer therapy. Additionally, the anti-inflammatory effects of CBE-ZnO-NPs were evident in LPS-induced RAW 264.7 cells, with an IC₅₀ value of 69.3 µg/mL, indicating their ability to modulate inflammatory responses. The green synthesis approach not only enhances the biocompatibility and stability of the nanoparticles but also aligns with the growing demand for sustainable and eco-friendly nanomaterial production. The integration of bioactive compounds from clove buds, such as eugenol, into the nanoparticle synthesis process further enhances their therapeutic potential. This study underscores the importance of plant-derived nanomaterials in addressing critical biomedical challenges, including cancer, bacterial infections, and inflammatory disorders. Future research should focus on optimizing the synthesis process, exploring in vivo efficacy, and elucidating the molecular mechanisms underlying the observed biological activities. The findings pave the way for the development of next-generation nanotherapeutics with enhanced safety, efficacy, and environmental sustainability.

Acknowledgment

The authors would like to acknowledge the Deanship of the Graduate Studies and Scientific Research, Taif University, for funding this work.

Disclosure

The authors declare no conflict of interest in this work.

References

1. Aliero AS, Hasmoni SH, Haruna A, Isah M, Malek NA, Zawawi NA. Bibliometric exploration of green synthesized silver nanoparticles for antibacterial activity. *Emerg Contam.* **2025**;11(1):100411.
2. Khalil MA, El-Shanshoury AE, Alghamdi MA, et al. Biosynthesis of silver nanoparticles by marine actinobacterium *Nocardiopsis dassonvillei* and exploring their therapeutic potentials. *Front Microbiol.* **2022**;12:705673. doi:10.3389/fmicb.2021.705673
3. Ali SS, Zagklis D, Kornaros M, Sun J. Cobalt oxide nanoparticles as a new strategy for enhancing methane production from anaerobic digestion of noxious aquatic weeds. *Bioresour Technol.* **2023**;368:128308. doi:10.1016/j.biortech.2022.128308
4. Khalil MA, El Maghraby GM, Sonbol FI, Allam NG, Ateya PS, Ali SS. Enhanced efficacy of some antibiotics in presence of silver nanoparticles against multidrug resistant *Pseudomonas aeruginosa* recovered from burn wound infections. *Front Microbiol.* **2021**;12:648560. doi:10.3389/fmicb.2021.648560
5. Ali SS, Al-Tohamy R, Koutra E, et al. Nanobiotechnological advancements in agriculture and food industry: applications, nanotoxicity, and future perspectives. *Sci Total Environ.* **2021**;792:148359. doi:10.1016/j.scitotenv.2021.148359
6. Ying S, Guan Z, Ofogebu PC, et al. Green synthesis of nanoparticles: current developments and limitations. *Environ Technol Innov.* **2022**;26:102336. doi:10.1016/j.eti.2022.102336
7. Ali SS, Morsy R, El-Zawawy NA, Fareed MF, Bedaiwy MY. Synthesized zinc peroxide nanoparticles (ZnO₂-NPs): a novel antimicrobial, anti-elastase, anti-keratinase, and anti-inflammatory approach toward polymicrobial burn wounds. *Int J Nanomed.* **2017**;12:6059–6073. doi:10.2147/IJN.S141201
8. Sobhy M, Ali SS, Khalil MA, et al. Exploring the potential of zinc oxide nanoparticles against pathogenic multi-drug resistant *Staphylococcus aureus* from ready-to-eat meat and its proposed mechanism. *Food Control.* **2024**;156:110117. doi:10.1016/j.foodcont.2023.110117
9. Ali SS, Sonbol FI, Sun J, et al. Molecular characterization of virulence and drug resistance genes-producing *Escherichia coli* isolated from chicken meat: metal oxide nanoparticles as novel antibacterial agents. *Microb Pathog.* **2020**;143:104164. doi:10.1016/j.micpath.2020.104164
10. Ali SS, Moawad MS, Hussein MA, et al. Efficacy of metal oxide nanoparticles as novel antimicrobial agents against multi-drug and multi-virulent *Staphylococcus aureus* isolates from retail raw chicken meat and giblets. *Int J Food Microbiol.* **2021**;344:109116. doi:10.1016/j.ijfoodmicro.2021.109116
11. Sobhy M, Ali SS, Cui H, Lin L, El-Sapagh S. Exploring the potential of 1,8-cineole from cardamom oil against food-borne pathogens: antibacterial mechanisms and its application in meat preservation. *Microb Pathog.* **2023**;184:106375. doi:10.1016/j.micpath.2023.106375
12. Raha S, Ahmaruzzaman M. ZnO nanostructured materials and their potential applications: progress, challenges and perspectives. *Nanoscale Adv.* **2022**;4(8):1868–1925. doi:10.1039/d1na00880c
13. Al-Darwesh MY, Ibrahim SS, Mohammed MA. A review on plant extract mediated green synthesis of zinc oxide nanoparticles and their biomedical applications. *Results Chem.* **2024**;7:101368.
14. Gul M, Kashif M, Shahid K. Eco-friendly approaches in the synthesis of ZnO nanoparticles using plant extract: a review. *Phytopharmacol Res J.* **2024**;3(2):1–25.
15. Jain A, Bhise K. Green synthesis methods for metallic zinc oxide nanoparticles: a sustainable angle. In: *Synthesizing and Characterizing Plant-Mediated Biocompatible Metal Nanoparticles*. IGI Global; **2025**:63–90.
16. Hamed R, Obeid RZ, Abu-Huwajir R. Plant mediated-green synthesis of zinc oxide nanoparticles: an insight into biomedical applications. *Nanotechnol Rev.* **2023**;12(1):20230112. doi:10.1515/ntrev-2023-0112
17. Vaou N, Stavropoulou E, Voidarou C, Tsigalou C, Bezirtzoglou E. Towards advances in medicinal plant antimicrobial activity: a review study on challenges and future perspectives. *Microorganisms.* **2021**;9(10):2041. doi:10.3390/microorganisms9102041
18. Nguyen DT, Van Tran T, Nguyen TT, Nguyen DH, Alhassan M, Lee T. New frontiers of invasive plants for biosynthesis of nanoparticles towards biomedical applications: a review. *Sci Total Environ.* **2023**;857:159278. doi:10.1016/j.scitotenv.2022.159278
19. Puri A, Mohite P, Maitra S, et al. From nature to nanotechnology: the interplay of traditional medicine, green chemistry, and biogenic metallic phytonanoparticles in modern healthcare innovation and sustainability. *Biomed Pharmacother.* **2024**;170:116083. doi:10.1016/j.biopha.2023.116083
20. Batiha GE, Alkazmi LM, Wasef LG, Beshbishy AM, Nadwa EH, Rashwan EK. *Syzygium aromaticum* L. (Myrtaceae): traditional uses, bioactive chemical constituents, pharmacological and toxicological activities. *Biomolecules.* **2020**;10(2):202. doi:10.3390/biom10020202
21. Xue Q, Xiang Z, Wang S, Cong Z, Gao P, Liu X. Recent advances in nutritional composition, phytochemistry, bioactive, and potential applications of *Syzygium aromaticum* L. *Front Nutr.* **2022**;9:1002147. doi:10.3389/fnut.2022.1002147
22. Haiouani K, Hegazy S, Alsaedi H, Bechelany M, Barhoum A. Green synthesis of hexagonal-like ZnO nanoparticles modified with phytochemicals of clove (*Syzygium aromaticum*) and *Thymus capitatus* extracts: enhanced antibacterial, antifungal, and antioxidant activities. *Materials.* **2024**;17(17):4340. doi:10.3390/ma17174340
23. Vairamuthu S, Sampath S, Sravanthy G, et al. Clove mediated synthesis of Ag-ZnO doped fucoidan nanocomposites and their evaluation of antibacterial, antioxidant, and cytotoxicity efficacy study. *Results Chem.* **2024**;11:101783. doi:10.1016/j.rechem.2024.101783
24. Malik K, Kazmi A, Sultana T, et al. A mechanistic overview on green assisted formulation of nanocomposites and their multifunctional role in biomedical applications. *Heliyon.* **2025**;11(1):e12345.
25. Ahmed B, Solanki B, Zaidi A, Khan MS, Musarrat J. Bacterial toxicity of biomimetic green zinc oxide nanoantibiotic: insights into ZnONP uptake and nanocolloid–bacteria interface. *Toxicol Res.* **2019**;8(2):246–261. doi:10.1039/C8TX00267C
26. Nawaz A, Farhan A, Maqbool F, et al. Zinc oxide nanoparticles: pathways to micropollutant adsorption, dye removal, and antibacterial actions—a study of mechanisms, challenges, and future prospects. *J Mol Struct.* **2024**;1301:138545. doi:10.1016/j.molstruc.2024.138545
27. Abebe B, Zereffa EA, Tadesse A, Murthy HA. A review on enhancing the antibacterial activity of ZnO: mechanisms and microscopic investigation. *Nanoscale Res Lett.* **2020**;15(1):1–9. doi:10.1186/s11671-020-03418-6
28. Murali M, Kalegowda N, Gowtham HG, et al. Plant-mediated zinc oxide nanoparticles: advances in the new millennium towards understanding their therapeutic role in biomedical applications. *Pharmaceutics.* **2021**;13(10):1662. doi:10.3390/pharmaceutics13101662
29. Sanati M, Afshari AR, Kesharwani P, Sukhorukov VN, Sahebkar A. Recent trends in the application of nanoparticles in cancer therapy: the involvement of oxidative stress. *J Control Release.* **2022**;348:287–304. doi:10.1016/j.jconrel.2022.05.035
30. Naser SS, Ghosh B, Simnani FZ, et al. Emerging trends in the application of green synthesized biocompatible ZnO nanoparticles for translational paradigm in cancer therapy. *J Nanotheranostics.* **2023**;4(3):248–279. doi:10.3390/jnt4030012

31. Tayyeb JZ, Priya M, Guru A, et al. Multifunctional curcumin mediated zinc oxide nanoparticle enhancing biofilm inhibition and targeting apoptotic specific pathway in oral squamous carcinoma cells. *Mol Biol Rep.* 2024;51(1):423. doi:10.1007/s11033-024-09407-7
32. Al-Asfour A, Bhardwaj RG, Karched M. Growth suppression of oral squamous cell carcinoma cells by *Lactobacillus acidophilus*. *Int Dent J.* 2024;74(5):1151–1160. doi:10.1016/j.identj.2024.03.017
33. Marco I, Feyerabend F, Willumeit-Römer R, Van der Biest O. Degradation testing of Mg alloys in Dulbecco's modified Eagle medium: influence of medium sterilization. *Mater Sci Eng C.* 62:68–78. doi:10.1016/j.msec.2016.01.039
34. Taciak B, Białasek M, Braniewska A, et al. Evaluation of phenotypic and functional stability of RAW 264.7 cell line through serial passages. *PLoS One.* 2018;13(6):e0198943. doi:10.1371/journal.pone.0198943
35. Wang S, Xiao L, Prasadam I, et al. Inflammatory macrophages interrupt osteocyte maturation and mineralization via regulating the Notch signaling pathway. *Mol Med.* 2022;28(1):102. doi:10.1186/s10020-022-00530-4
36. Hussien NA. Antimicrobial potential of biosynthesized zinc oxide nanoparticles using banana peel and date seeds extracts. *Sustainability.* 2023;15:9048. doi:10.3390/su15119048
37. Abdelmigid HM, Hussien NA, Alyamani AA, Morsi MM, AlSufyani NM, Kadi HA. Green synthesis of zinc oxide nanoparticles using pomegranate fruit peel and solid coffee grounds vs. chemical method of synthesis, with their biocompatibility and antibacterial properties investigation. *Molecules.* 2022;27:1236. doi:10.3390/molecules27041236
38. Hussien NA, Al Malki JS, Al Harthy FAR, Mazi AW, Al Shadadi JAA. Sustainable eco-friendly synthesis of zinc oxide nanoparticles using banana peel and date seed extracts, characterization, and cytotoxicity evaluation. *Sustainability.* 2023;15:9864. doi:10.3390/su15139864
39. El-Belely EF, Farag MMS, Said HA, et al. Green synthesis of zinc oxide nanoparticles (ZnO-NPs) using *Arthrospira platensis* (Class: cyanophyceae) and evaluation of their biomedical activities. *Nanomaterials.* 2021;11:95. doi:10.3390/nano11010095
40. Mohamed HRH, Hussien NA. GC-MS analysis and molecular docking studies of *Lavandula dentata* leaves extract of Taif region, Saudi Arabia. *Indian J Anim Res.* 2024;58(10):1677–1687. doi:10.18805/IJAR.BF-1808
41. Ayoola GA, Lawore FM, Adelowotan T, et al. Chemical analysis and antimicrobial activity of the essential oil of *Syzygium aromaticum* (clove). *Afr J Microbiol Res.* 2008;2:162–166.
42. Goel N, Ahmad R, Singh R, Sood S, Khare SK. Biologically synthesized silver nanoparticles by *Streptomyces* sp. EMB24 extracts used against the drug-resistant bacteria. *Bioresour Technol Rep.* 2021;15:100753. doi:10.1016/j.biteb.2021.100753
43. Krishnamoorthy R, Yehia HM, Abdul Hameed MM, et al. Ultrasonic-assisted food grade nanoemulsion preparation from clove bud essential oil and evaluation of its antioxidant and antibacterial activity. *Green Process Synth.* 2022;11(1):974–986. doi:10.1515/gps-2022-0083
44. Zhou M, Wei Z, Qiao H, Zhu L, Yang H, Xia T. Particle size and pore structure characterization of silver nanoparticles prepared by confined arc plasma. *Nanomaterials.* 2009;1:968058. doi:10.1155/2009/968058
45. Mansour AT, Alprol AE, Khedawy M, et al. Green synthesis of zinc oxide nanoparticles using red seaweed for the elimination of organic toxic dye from an aqueous solution. *Mater.* 2022;15(15):5169. doi:10.3390/ma15155169
46. Kim C, Le D, Lee M. Diterpenoids isolated from *Podocarpus macrophyllus* inhibited the inflammatory mediators in LPS-induced HT-29 and RAW 264.7 cells. *Molecules.* 2021;26(14):4326. doi:10.3390/molecules26144326
47. Skehan P, Storeng R, Scudiero D, et al. New colorimetric cytotoxicity assay for anticancer-drug screening. *J Natl Cancer Inst.* 1990;82(13):1107–1112. doi:10.1093/jnci/82.13.1107
48. Allam RM, Al-Abd AM, Khedr A, et al. Fingolimod interrupts the crosstalk between estrogen metabolism and sphingolipid metabolism within prostate cancer cells. *Toxicol Lett.* 2018;291:77–85. doi:10.1016/j.toxlet.2018.04.008
49. van der Linde K, Lim BT, Rondeel JM, Antonissen LP, de Jong GM. Improved bacteriological surveillance of haemodialysis fluids: a comparison between tryptic soy agar and reasoner's 2A media. *Nephrol Dial Transplant.* 1999;14(10):2433–2437. doi:10.1093/ndt/14.10.2433
50. Clinical and Laboratory Standards Institute (CLSI). *Performance Standards for Antimicrobial Susceptibility Tests. CLSI Standard M02.* 13th ed. Wayne, PA: Clinical and Laboratory Standards Institute; 2018.
51. Ahmed AH, Mohamed MFA, Allam RM, et al. Design, synthesis, and molecular docking of novel pyrazole-chalcone analogs of Isoniazid as 5-LOX, iNOS and tubulin polymerization inhibitors with potential anticancer and anti-inflammatory activities. *Bioorg Chem.* 2022;129:106171. doi:10.1016/j.bioorg.2022.106171
52. Syahida A, Israf DA, Lajis NH, et al. Effect of compounds isolated from natural products on IFN- γ /LPS-induced nitric oxide production in RAW 264.7 macrophages. *Pharm Biol.* 2006;44(1):50–59. doi:10.1080/13880200500530765
53. Chen X, Ren L, Li M, Qian J, Fan J, Du B. Effects of clove essential oil and eugenol on quality and browning control of fresh-cut lettuce. *Food Chem.* 2017;214:432–439. doi:10.1016/j.foodchem.2016.07.101
54. Sheweita SA, El-Hosseiny LS, Nashashibi MA. Protective effects of essential oils as natural antioxidants against hepatotoxicity induced by cyclophosphamide in mice. *PLoS One.* 2016;11:e0165667.
55. Ali S, Prasad R, Mahmood A, et al. Eugenol-rich fraction of *Syzygium aromaticum* (clove) reverses biochemical and histopathological changes in liver cirrhosis and inhibits hepatic cell proliferation. *J Cancer Prev.* 2014;19:288–300. doi:10.15430/JCP.2014.19.4.288
56. Mohanta YK, Behera SK. Biosynthesis, characterization and antimicrobial activity of silver nanoparticles by *Streptomyces* sp. SS2. *Bioprocess Biosyst Eng.* 2014;37:2263–2269. doi:10.1007/s00449-014-1205-6
57. Shanmugaiah V, Harikrishnan HS, Al-Harbi NS, Shine K, Khaled JM. Facile synthesis of silver nanoparticles using *Streptomyces* sp. VSMGT1014 and their antimicrobial efficiency. *Dig J Nanomater Biostruct.* 2015;10:179–187.
58. Karthik L, Kumar G, Vishnu Kirthi A, Rahuman AA, Rao KVB. *Streptomyces* sp. LK3 mediated synthesis of silver nanoparticles and its biomedical application. *Bioprocess Biosyst Eng.* 2014;37:261–267. doi:10.1007/s00449-013-0994-3
59. Ng J, Cheung W, McKay G. Equilibrium studies of the sorption of Cu(II) ions onto chitosan. *J Colloid Interface Sci.* 2002;255:64–74. doi:10.1006/jcis.2002.8664
60. Wahab R, Kim YS, Shin HS. Fabrication, characterization and growth mechanism of heterostructured zinc oxide nanostructures via solution method. *Curr Appl Phys.* 2011;11:334–340. doi:10.1016/j.cap.2010.07.030
61. Pandimurugan R, Thambidurai S. Novel seaweed capped ZnO nanoparticles for effective dye photodegradation and antibacterial activity. *Adv Powder Technol.* 2016;27:1062–1072. doi:10.1016/j.appt.2016.03.014
62. Batterjee MG, Nabi A, Kamli MR, Alzahrani KA, Danish EY, Malik MA. Green hydrothermal synthesis of zinc oxide nanoparticles for UV-light-induced photocatalytic degradation of ciprofloxacin antibiotic in an aqueous environment. *Catalysts.* 2022;12:1347. doi:10.3390/catal12111347

63. Modena MM, Rühle B, Burg TP, Wuttke S. Nanoparticle characterization: what to measure? *Adv Mater*. 2019;31:1970226. doi:10.1002/adma.201970226
64. Kalaba MH, El-Sherbiny GM, Ewais EA, et al. Green synthesis of zinc oxide nanoparticles (ZnO-NPs) by *Streptomyces baarnensis* and its active metabolite (Ka): a promising combination against multidrug-resistant ESKAPE pathogens and cytotoxicity. *BMC Microbiol*. 2024;24:254. doi:10.1186/s12866-024-03392-4
65. Badran M. Formulation and in vitro evaluation of flufenamic acid loaded deformable liposome for improved skin delivery. *Dig J Nanomater Biostruct*. 2014;9:83–91.
66. Putri DC, Dwiaastuti R, Marchaban M, Nugroho AK. Optimization of mixing temperature and sonication duration in liposome preparation. *J Pharm Sci Commun*. 2017;14:79–85. doi:10.24071/jpsc.142728
67. Yu L, Haley S, Perret J, Harris M, Wilson J, Qian M. Free radical scavenging properties of wheat extracts. *J Agric Food Chem*. 2002;50:1619–1624. doi:10.1021/jf010964p
68. Abdelbaky AS, El-Mageed TA A, Babalghith AO, Selim S, Mohamed AMH. Green synthesis and characterization of ZnO nanoparticles using *Pelargonium odoratissimum* (L.) aqueous leaf extract and their antioxidant, antibacterial and anti-inflammatory activities. *Antioxidants*. 2022;11(8):1444. doi:10.3390/antiox11081444
69. Vimala K, Sundarraj S, Paulpandi M, Vengatesan S, Kannan S. Green synthesized doxorubicin-loaded zinc oxide nanoparticles regulates the Bax and Bcl-2 expression in breast and colon carcinoma. *Process Biochem*. 2014;49:160–172.
70. Shamhari NM, Wee BS, Chin SF, Kok KY. Synthesis and characterization of zinc oxide nanoparticles with small particle size distribution. *Acta Chim Slov*. 2018;65(3). doi:10.17344/acs.2018.4213
71. Ismail MA, Taha KK, Modwi A, Khezami L. ZnO nanoparticles: surface and X-ray profile analysis. *J Ovonic Res*. 2018;14(5):381–393.
72. Seo SW, Kim K, Shin MR. Anti-inflammatory effect by cloves treatment in LPS-induced RAW264.7 cells. *Pharmacogn Mag*. 2023;19(1):105–116.
73. Ahmed RM, Esmaeil DAM, El-Nagdy SY, El-Sisi NA. Antitumoral properties of the pomegranate peel and blueberry extracts against tongue carcinoma (in vitro study). *Saudi Dent J*. 2023;35(8):985–995. doi:10.1016/j.sdentj.2023.07.021
74. Moghimi SM, Hunter AC, Murray JC. Long-circulating and target-specific nanoparticles: theory to practice. *Pharmacol Rev*. 2001;53:283–318.
75. Anjum S, Hashim M, Malik SA, et al. Recent advances in zinc oxide nanoparticles (ZnO NPs) for cancer diagnosis, target drug delivery, and treatment. *Cancers*. 2021;13(18):4570. doi:10.3390/cancers13184570
76. Yi GC, Wang C, Park WI. ZnO nanorods: synthesis, characterization and applications. *Semicond Sci Technol*. 2005.
77. Miao LG, Shi BM, Stanislaw N, Mu CM, Qi KZ. Facile synthesis of hierarchical ZnO microstructures with enhanced photocatalytic activity. *Mater Sci Poland*. 2017;35:45–49. doi:10.1515/msp-2017-0007
78. Summer M, Ashraf R, Ali S, et al. Inflammatory response of nanoparticles: mechanisms, consequences, and strategies for mitigation. *Chemosphere*. 2024;11:142826. doi:10.1016/j.chemosphere.2024.142826
79. Naeem A, Hu P, Yang M, et al. Natural products as anticancer agents: current status and future perspectives. *Molecules*. 27(23):8367. doi:10.3390/molecules27238367
80. Wang H, Wingett D, Engelhard M, et al. Fluorescent dye encapsulated ZnO particles with cell-specific toxicity for potential use in biomedical applications. *J Mater Sci Mater Electron*. 2008;20:11–22. doi:10.1007/s10856-008-3541-z
81. Hanley C, Layne J, Punnoose A, et al. Preferential killing of cancer cells and activated human T cells using ZnO nanoparticles. *Nanotechnology*. 2008;19:295103. doi:10.1088/0957-4484/19/29/295103
82. Abbasi BA, Iqbal J, Ahmad R, et al. Bioactivities of *Geranium wallichianum* leaf extracts conjugated with zinc oxide nanoparticles. *Biomolecules*. 2019;10(1):38. doi:10.3390/biom10010038
83. Motelica L, Oprea OC, Vasile BS, et al. Antibacterial activity of solvothermal obtained ZnO nanoparticles with different morphology and photocatalytic activity against a dye mixture: methylene blue, rhodamine B, and methyl Orange. *Int J mol Sci*. 2023;24(6):5677. doi:10.3390/ijms24065677
84. Sánchez-López E, Gomes D, Esteruelas G, et al. Metal-based nanoparticles as antimicrobial agents: an overview. *Nanomaterials*. 2020;10(2):292. doi:10.3390/nano10020292
85. Kim I, Viswanathan K, Kasi G, Thanakkasaranee S, Sadeghi K, Seo J. ZnO nanostructures in active antibacterial food packaging: preparation methods, antimicrobial mechanisms, safety issues, future prospects, and challenges. *Food Rev Int*. 2022;38(4):537–565. doi:10.1080/87559129.2020.1737709
86. Jiang S, Lin K, Cai M. ZnO nanomaterials: current advancements in antibacterial mechanisms and applications. *Front Chem*. 2020;8:580. doi:10.3389/fchem.2020.00580
87. Choudhury M, Bindra HS, Singh K, Singh AK, Nayak R. Antimicrobial polymeric composites in consumer goods and healthcare sector: a healthier way to prevent infection. *Polym Adv Technol*. 2022;33(7):1997–2024. doi:10.1002/pat.5660
88. Zahoor S, Sheraz S, Shams DF, et al. Biosynthesis and anti-inflammatory activity of zinc oxide nanoparticles using leaf extract of *Senecio chrysanthemoides*. *Biomed Res Int*. 2023;2023:3280708. doi:10.1155/2023/3280708
89. Gojani EG, Wang B, Li DP, Kovalchuk O, Kovalchuk I. Anti-inflammatory properties of eugenol in lipopolysaccharide-induced macrophages and its role in preventing β -cell dedifferentiation and loss induced by high glucose-high lipid conditions. *Molecules*. 2023;28(22):7619. doi:10.3390/molecules28227619
90. Hamza M, Muhammad S, Zahoor SJA. Biologically synthesized zinc oxide nanoparticles and its effect—a review. *Acta Sci Appl Phys*. 2022;2(9).
91. Siddiqi KS, Ur Rahman A, Tajuddin H, Husen A. Properties of zinc oxide nanoparticles and their activity against microbes. *Nanoscale Res Lett*. 2018;13(1):141. doi:10.1186/s11671-018-2532-3
92. Beegam A, Prasad P, Jose J, et al. *Toxicology—new Aspects to This Scientific Conundrum Environmental Fate of Zinc Oxide Nanoparticles: Risks and Benefits*. Vol. 33. IntechOpen; 2016.
93. Al Lawati H, Jamali F. Onset of action and efficacy of ibuprofen liquiset as compared to solid tablets: a systematic review and meta-analysis. *J Pharm Pharm Sci*. 2016;19(3):301–311. doi:10.18433/J3B897
94. Prasad LK, O'Mary H, Cui Z. Nanomedicine delivers promising treatments for rheumatoid arthritis. *Nanomedicine*. 2015;10(13):2063–2074. doi:10.2217/nmm.15.45
95. Nagajyothi PC, Cha SJ, Yang IJ, Sreekanth TVM, Kim KJ, Shin HM. Antioxidant and anti-inflammatory activities of zinc oxide nanoparticles synthesized using *Polygala tenuifolia* root extract. *J Photochem Photobiol B*. 2015;146:10–17. doi:10.1016/j.jphotobiol.2015.02.008

International Journal of Nanomedicine**Publish your work in this journal**

The International Journal of Nanomedicine is an international, peer-reviewed journal focusing on the application of nanotechnology in diagnostics, therapeutics, and drug delivery systems throughout the biomedical field. This journal is indexed on PubMed Central, MedLine, CAS, SciSearch®, Current Contents®/Clinical Medicine, Journal Citation Reports/Science Edition, EMBase, Scopus and the Elsevier Bibliographic databases. The manuscript management system is completely online and includes a very quick and fair peer-review system, which is all easy to use. Visit <http://www.dovepress.com/testimonials.php> to read real quotes from published authors.

Submit your manuscript here: <https://www.dovepress.com/international-journal-of-nanomedicine-journal>

Dovepress
Taylor & Francis Group